

## ORIGINAL ARTICLE

# Effects of partial miscibility on the structure and properties of novel high performance blends composed of poly(*p*-phenylene sulfide) and poly(phenylsulfone)

Saori Nara and Hideko T Oyama

Although super-engineering plastics show superb thermal stabilities and long lifetime, their mechanical properties are often insufficient due to their molecular stiffness, as observed for poly(*p*-phenylene sulfide) (PPS). In the present study, a novel blend of two super-engineering plastics, PPS and poly(phenylsulfone) (PPSU), was investigated in detail. Differential scanning calorimetry and dynamic mechanical analysis (DMA) measurements revealed for the first time that the PPS/PPSU blends showed partial miscibility. The desirable interfacial adhesion achieved by the partial miscibility and the segmental mobility of PPSU, observed as a transition peak at approximately  $-100\text{ }^{\circ}\text{C}$  in the DMA measurements, most likely contributed to remedying the brittleness of PPS. Furthermore, small-angle X-ray scattering measurements revealed that the PPSU chains intruded into the amorphous region between the PPS lamellae during the crystallization of PPS as a result of the interlamellar segregation of the PPSU chains, which were partially miscible with PPS in the molten state. Thermogravimetric analysis measurements under a nitrogen atmosphere demonstrated that the thermal stabilities of PPS blends were significantly improved by the addition of PPSU.

*Polymer Journal* (2014) 46, 568–575; doi:10.1038/pj.2014.21; published online 23 April 2014

**Keywords:** blend; crystallization; mechanical and thermal properties; partial miscibility; poly(phenylsulfone); poly(*p*-phenylene sulfide)

## INTRODUCTION

Thermoplastic polymers can be classified into three groups depending on their thermal stability and mechanical properties: (i) commodity plastics, (ii) engineering plastics and (iii) super-engineering plastics.<sup>1,2</sup> Commodity plastics are those widely used in daily human life, such as polyolefins, polystyrene and poly(vinyl chloride), whose thermal stability in continuous usage for long time period is under  $100\text{ }^{\circ}\text{C}$ . Engineering plastics are usually categorized as thermoplastic polymers with tensile strengths  $>5\text{ kgf mm}^{-2}$ , whose thermal stabilities in continuous usage are over  $100\text{ }^{\circ}\text{C}$ , and which are represented by polyacetal, polyamides 6 and 66 (PA6, PA66), poly(butylene terephthalate), modified poly(phenylene ether) and polycarbonate (PC). Finally, super-engineering plastics are N-, S-, and O-containing polymers with tensile strengths  $>10\text{ kgf mm}^{-2}$ , whose thermal stabilities in continuous usage are over  $150\text{ }^{\circ}\text{C}$ , and which are represented by poly(arylate), poly(ether sulfone) (PES), poly(*p*-phenylene sulfide) (PPS), poly(ether ether ketone) (PEEK), polyimide and poly(ether imide).

In the development of thermally stable polymers, chemical stability is achieved by incorporating strong chemical bonds with high bond dissociation energies. ‘Super-engineering plastics’ with extremely high thermal stabilities possess stable chemical bonds in their main chains

with a stiff structure provided by aromatic rings.<sup>3</sup> Recently, the need for super-engineering plastics has significantly increased because of developments in technology, for example, aircraft, space rockets, automobiles, fuel cells and electric and electronic devices. Although super-engineering plastics show superb thermal stabilities and long lifetime, their mechanical properties are often insufficient due to their molecular stiffness, as observed for PPS.

To improve its physical properties, the modification of PPS by blending is a convenient solution. There have been various PPS blends reported in the literature; for example, PPS blends with polyamide,<sup>4–8</sup> thermotropic liquid crystal polymers (LCP),<sup>9,10</sup> elastomers,<sup>11,12</sup> poly(ether imide),<sup>13</sup> polyethylene,<sup>14</sup> PS,<sup>15</sup> poly(ethylene terephthalate) (PET),<sup>14</sup> polypropylene,<sup>16</sup> PC,<sup>17</sup> PES<sup>18,19</sup> and PEEK.<sup>20,21</sup> However, in most of these studies, the effects of blending on the crystallization of PPS were studied, but the effects on physical properties were not investigated.

Furthermore, PPS does not dissolve in any organic solvents under  $200\text{ }^{\circ}\text{C}$ , giving it excellent chemical resistance. Such characteristics hinder its solubility (that is, miscibility) with other polymers. However, Inoue and coworkers<sup>6</sup> observed that although the (80/20) PA 4,6/PPS blend is completely immiscible in the quiescent state, it becomes miscible under high shear flow (for example, above  $150\text{ s}^{-1}$

at 310 °C and 189 s<sup>-1</sup> at 320 °C), and ensuing phase separation proceeds via spinodal decomposition. This shear-induced miscibility was not observed for other compositions. Furthermore, two polymers have been reported to show partial miscibility with PPS; both are amorphous polymers, PC<sup>17</sup> and PES.<sup>18</sup> Here, the partial miscibility indicates that a part of one polymer component molecularly dissolves in the other polymer component and *vice versa* while the blend is phase separated. Wu *et al.*<sup>17</sup> prepared PPS/PC blends by melt blending and found partial miscibility between the component polymers from shifts of their tan  $\delta$  peaks measured by dynamic mechanical analysis (DMA). They also investigated non-isothermal crystallization behavior by differential scanning calorimetry (DSC), which suggested that the amorphous PC in the PPS/PC blend acts as a crystallization inhibitor for PPS. Furthermore, Shibata *et al.*<sup>18</sup> reported partial miscibility between PPS and PES from DSC measurements, which showed a linear reduction in the equilibrium melting point of PPS with increasing PES content. However, in these studies, the structure and mechanical properties of the obtained blends were not investigated.

Because PPS generates completely immiscible blends with other polymers in most cases, several studies have been conducted to examine the effectiveness of compatibilizers, which stabilize the interfaces of blends with phase-separated morphologies; examples include ethylene-maleic anhydride-glycidyl methacrylate terpolymer,<sup>4</sup> poly(ethylene-stat-methacrylate)<sup>5</sup> and maleic anhydride-grafted SEBS<sup>8</sup> for PPS/PA66, maleic anhydride-grafted polypropylene for PPS/LCD<sup>9</sup> and polymerizable monomeric reactant-polyimide for PPS/PES.<sup>19</sup>

This study reports the production of novel super-engineering blends composed of a crystalline super-engineering plastic, PPS, and an amorphous super-engineering plastic, poly(phenylsulfone) (PPSU), without the use of a compatibilizer. PPSU is a new material in the family of super-engineering plastics that contains a diphenylsulfonyl group and an ether group, as shown in Figure 1. It is known that the sulfur atom in the diphenylsulfonyl group is in the highest oxidation state and that the sulfonyl group attracts electrons from the adjacent phenyl rings and also prevents the phenyl rings from rotating.<sup>2</sup> As a result, the strong resonance structure of the para-linked diphenylsulfonyl group enhances the thermal stability of the molecule, and its steric hindrance prevents the polymer from crystallizing. Because of these characteristics, the diphenylsulfonyl group has an anti-oxidation function, preventing oxidants from receiving electrons. The ether group in PPSU gives flexibility to the molecule and thereby improves its processability. As a result, PPSU is an amorphous polymer with an extremely high  $T_g$  of ~220 °C, a high modulus, and excellent thermal stability. Furthermore, the extremely high thermal stability of PPSU also contributes to flame retardation, as shown by its limiting oxygen index of 32. (Reported by the BASF

manufacturer.) PPSU is also very unique in that it displays an outstanding impact strength of 65 kJ m<sup>-2</sup>, as measured by the Charpy impact test (ISO179 procedure) using a notched specimen at 23 °C. (Reported by the BASF manufacturer.)

Although there are a very limited number of studies on PPSU blends, it has been reported that PPSU is miscible with polyimide or poly(amide-imide).<sup>22</sup> Shifts in the two  $T_g$  values were also observed upon blending in PPSU/PET, which was attributed to a chemical reaction, presumably between the carbonyl groups of PET and the end groups of PPSU and not due to partial miscibility.<sup>23</sup> A study of immiscible PPSU blends included the incorporation of a small amount of silylated and sulfonated PPSU to sulfonated PEEK; the potential of the blends as proton-conducting membranes for batteries was investigated.<sup>24</sup> Furthermore, the application of PPSU blends as a gas permeation membrane<sup>25</sup> and foaming under high pressure CO<sub>2</sub> gas<sup>26</sup> have also been investigated.

To our knowledge, no study concerning PPS/PPSU blends has been reported in the literature until now. It was expected that the superior thermal stability of both component polymers would be maintained in the blends and that the incorporation of PPSU would improve the mechanical properties of PPS. In the present work, the effects of blending on the crystallization of PPS and the resulting thermal and mechanical properties were elucidated. It was revealed that PPS has partial miscibility with PPSU and that this affects the mechanical properties of the blend. The structures of the blends were investigated by TEM and SAXS, and the properties were studied by DSC, DMA, thermogravimetric analysis (TGA) and tensile tests.

## EXPERIMENTAL PROCEDURE

### Materials and sample preparation

Linear type PPS was obtained from the Kureha Corporation, Japan (grade name Fortron KPS W220A), and PPSU was kindly provided by the BASF Corporation, Germany (grade name of Ultrason P3010); both were used as received. Our DSC analysis estimated that the glass transition ( $T_g$ ) and melting temperatures ( $T_m$ ) of crystalline PPS were 85 °C and 278 °C, respectively and that the  $T_g$  of amorphous PPSU was 220 °C. The density of both polymers was reported to be 1.3 g cm<sup>-3</sup> by the manufacturers. Figure 1 shows the chemical structures of PPS and PPSU used in the present study.

PPS and PPSU were dried under vacuo overnight at 130 °C. Then, the polymers at given compositions were melt-mixed in a twin blade mixer (Toyo Seiki, KF70 V2, Tokyo, Japan) attached to a motor and a controller (Toyo Seiki, Labo Plastomill 4 M150) at 320 °C with a rotation speed of 100 r.p.m. for 10 min. Film specimens with dimensions of 90 mm × 90 mm × 500  $\mu$ m were prepared by hot pressing at 330 °C, quickly followed by a cold press at 20 °C or a quenching in ice water.

### Structure and thermal properties

The blend morphology was investigated by transmission electron microscopy (TEM) using a Philips Tecnai 30 microscope (FEI Company, Hillsboro, OR, USA) at an acceleration voltage of 300 kV. The samples were first exposed to ruthenium tetroxide (RuO<sub>4</sub>) vapor and then microtomed at room temperature prior to the TEM measurements.

Small-angle X-ray scattering (SAXS) measurements of the film specimens were performed with the Nano-viewer SAXS spectrometer manufactured by Rigaku, Tokyo, Japan, with monochromatic Cu K <sub>$\alpha$</sub>  radiation (0.154 nm) operated at 1.2 kW.

DSC was carried out with a calorimeter (TA Instruments, DSC-Q200, New Castle, DE, USA) at a heating rate of 10 °C min<sup>-1</sup> under nitrogen atmosphere in a temperature range between 40 and 300 °C. The net degree of crystallization ( $X_c$ ) of the PPS component in the blends was calculated by the following equation using the DSC results:

$$X_c(\%) = \frac{\Delta H_m \Delta H_c}{W \Delta H_f} \times 100 \quad (1)$$

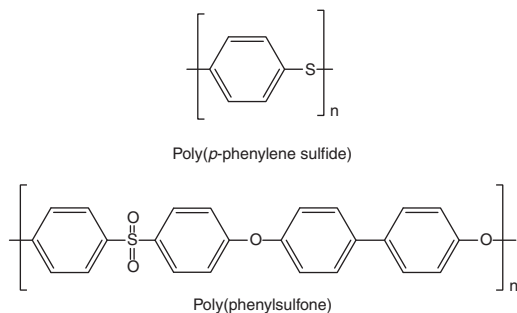


**Figure 1** Chemical structures of PPS and PPSU.

where  $W$  is the wt% of PPS in the blend and  $\Delta H_m$  and  $\Delta H_c$  are the enthalpies of melting and crystallization of the samples, respectively, with the theoretical heat of fusion for fully crystallized PPS,  $\Delta H_f$ , obtained from the literature,  $12.1 \text{ kJ mol}^{-1}$ .<sup>27</sup>

DMA was performed with an instrument (Rheovibron DDV-01FP-W, A & D, Tokyo, Japan) with an oscillatory frequency of 1 Hz in tensile mode. During the measurements, the specimens were heated from 150 to 300 °C at  $2^\circ\text{C min}^{-1}$ .

### Mechanical tests

Tensile tests of the film specimens with  $\sim 0.5 \text{ mm}$  thickness were performed following the ISO 527 procedure at room temperature (Strograph VES-50D, Toyo Seiki) with a tensile speed of  $10 \text{ mm min}^{-1}$ .<sup>28</sup> The same measurements were repeated at least five times, and the results were averaged.

## RESULTS AND DISCUSSION

### Structure of PPS/PPSU

Figure 2 shows a TEM micrograph of (70/30) PPS/PPSU stained by  $\text{RuO}_4$  vapor, in which the matrix is crystalline PPS with a bumpy appearance due to the lamellae and the domain is amorphous PPSU with a smooth appearance. It has been reported that the terminal group of PPS can be altered depending on the synthetic method and solvents used in the process and that it can consist of  $-\text{Cl}$ ,  $-\text{SH}$ ,  $-\text{SNa}$ , the *N*-alkylamino group or the amino group.<sup>29</sup> Furthermore, in a study of PPSU (Radel R-5000, Solvay, S. A., Brussels, Belgium) blends with PET, it was speculated from the FTIR measurements that a reaction between the component polymers occurred, presumably between the terminal group of the PPSU and the carbonyl group of the polyester.<sup>23</sup> However, in the present study, the TEM results showing circular domains with a size greater than  $1 \mu\text{m}$  imply that the interfacial tension is high without the presence of any emulsifier at the interface.<sup>30</sup> Therefore, it is speculated that there is no interfacial reaction between PPS and PPSU, which generates emulsifiers.

Figure 3 shows DSC thermograms of quenched PPS/PPSU blends with various compositions and their component polymers measured at a heating rate of  $10^\circ\text{C min}^{-1}$ . The values of their  $T_g$ ,  $T_m$  and cold crystallization temperatures ( $T_{cc}$ ) are separately summarized in Table 1. All samples were solidified by quick immersion into ice water from the molten state in order to minimize the effects of the crystallization of PPS on the  $T_g$ . It was found that there are two

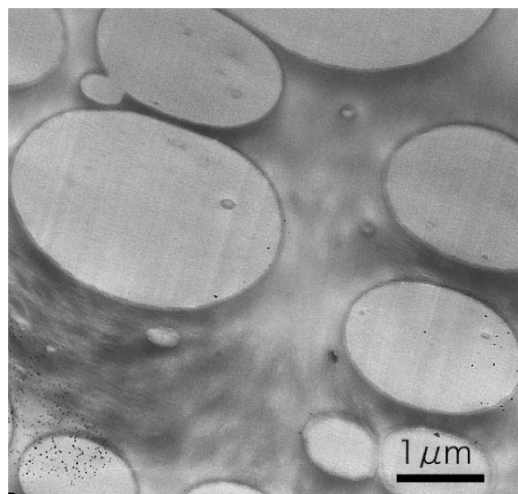


Figure 2 TEM micrograph of (70/30) PPS/PPSU stained by  $\text{RuO}_4$ .

distinct  $T_g$ 's in the DSC thermograms of the blends, which originate from the two component polymers, indicating immiscibility between PPS and PPSU. However, it was observed that the  $T_g$  of PPS shifted to a higher temperature (by  $3\text{--}5^\circ\text{C}$ ) and that the  $T_g$  of PPSU shifted to a lower temperature (by  $4\text{--}5^\circ\text{C}$ ) in the blends compared with the  $T_g$ 's of the neat polymers. These results indicate that both PPS and PPSU have limited solubility in the other component, thus having partial miscibility. Figure 3 also shows that the cold crystallization temperature,  $T_{cc}$ , of PPS tends to increase along with a significant decrease in the peak area of  $T_{cc}$  and  $T_m$  upon the addition of PPSU.

The shifts in the  $T_g$  values of the two component polymers in the blends were also verified by DMA measurements, as shown in Figures 4a and b. Because the films quenched in ice water used for the DSC measurements were not flat enough for the DMA measurements, the molten samples obtained in a hot press were solidified in a cold press at  $20^\circ\text{C}$  for the DMA measurements. As a result, the crystallinity of the neat PPS used for the DMA measurements was as high as 31%, although that of the quenched PPS used for the DSC measurements was as low as 5.9%. However, upon the addition of PPSU, the net PPS crystallinity of the blends solidified in the cold press in a similar manner was significantly reduced to below 10%. In Figure 4a showing the  $\tan \delta$  peaks in the temperature range close to

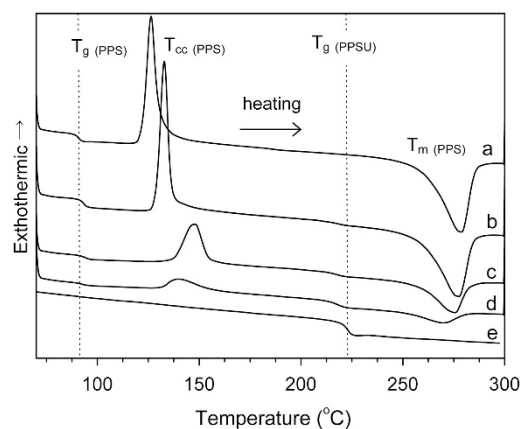


Figure 3 DSC thermograms of quenched PPS, PPSU and PPS/PPSU blends measured at a heating rate of  $10^\circ\text{C min}^{-1}$  ((PPS)/(PPSU) weight ratio of (a) (100/0), (b) (70/30), (c) (50/50), (d) (30/70), (e) (0/100)).

Table 1 Thermal properties of quenched PPS, PPSU and their blends measured by DSC at the heating rate of  $10^\circ\text{C min}^{-1}$

Sample	Thermal properties <sup>a</sup>				Crystallinity <sup>b</sup> (%)
	$T_g$ (PPS) (°C)	$T_{cc}$ (PPS) (°C)	$T_g$ (PPSU) (°C)	$T_m$ (PPS) (°C)	
PPS	89	126	—	279	5.9
PPSU	—	—	222	—	—
(70/30) PPS/PPSU	93	133	218	277	5.9
(50/50) PPS/PPSU	94	148	217	276	3.3
(30/70) PPS/PPSU	92	140	218	270	1.4

Abbreviations: PPS, poly(*p*-phenylene sulfide); PPSU, poly(phenylsulfone).

<sup>a</sup>Glass transition temperature ( $T_g$ ), cold crystallization temperature ( $T_{cc}$ ) and melting point ( $T_m$ ) were determined by their heat flow curves of DSC.

<sup>b</sup>Net crystallinity of PPS calculated by Equation (1) assuming the theoretical heat of fusion for fully crystallized PPS,  $\Delta H_f = 12.1 \text{ kJ mol}^{-1}$ .<sup>27</sup> These samples were quickly solidified in ice water from the melt.

$T_g(\text{PPS})$ , the peaks in neat PPS (a) and in the blends (b, c) ascribed to  $T_g$  were severely affected by crystallites already present prior to the DMA measurements and by further crystallization of PPS provoked by heating during the measurements. This resulted in ambiguity in the estimate of  $T_g(\text{PPS})$  by the DMA measurements. In contrast, it was easier to estimate the  $T_g$  of amorphous PPSU,  $T_g(\text{PPSU})$ , from the  $\tan \delta$  peak in Figure 4b, which gradually shifted toward lower temperatures with increasing PPS concentration; for example, from 233 °C for neat PPSU to 226 °C for (70/30) PPS/PPSU.

Unlike the DSC results, the decrease in  $T_g(\text{PPSU})$  upon the addition of PPS was composition dependent when the  $T_g(\text{PPSU})$  was estimated from the  $\tan \delta$  peak position in the DMA measurements. Furthermore, the temperature dependence of the storage modulus,  $E'$ , is also given in Figures 4c and d. The  $E'$  of the blends decreased at the  $T_g(\text{PPS})$  of  $\sim 95$  °C and at the  $T_g(\text{PPSU})$  of  $\sim 220$  °C. However, a significant increase in  $E'$  was observed at 120–130 °C in the (70/30) and (50/50) PPS/PPSU blends, which was caused by the cold crystallization of the PPS component during the heating process in the DMA measurements. The peculiar behaviors caused by crystallization were not observed for the neat PPS in Figures 4a and c because the neat PPS film used for the measurement had a high crystallinity of 31%. On the contrary, the (70/30) and (50/50) PPS/PPSU blends had much lower crystallinities, that is, 7.4% and 5.7%, respectively, which left the blends room to crystallize during the heating process in the measurements. The partial miscibility between PPS and PPSU significantly suppressed the crystallization of PPS, so that the neat PPS crystallized more easily compared with the PPS in the blends.

In the literature, it has been reported that PPS is partially miscible with PC<sup>17</sup> and PES.<sup>18</sup> In a study of the non-isothermal crystallization behavior of PPS/PC blends, it was reported that the addition of PC decreases the PPS overall crystallization rate because of the higher

viscosity of PC and/or the partial miscibility of the blends.<sup>17</sup> In the DSC results for the PPS/PES blends, the  $T_{cc}$  of the blended PPS at various compositions increased by a maximum of 4 °C compared with that of neat PPS,<sup>18</sup> whereas it increased more significantly in the present blends, by as much as 22 °C.

### Mechanical properties

The mechanical properties of the blends were investigated using tensile tests, as shown in Figure 5 and Table 2. Kolařík *et al.*<sup>31</sup> proposed a method to evaluate the interfacial adhesion of binary blends using the following equations, and the method has been applied to various blends.<sup>32</sup> For a blend with an interfacial adhesion strong enough to ensure stress transfer between the phases, an

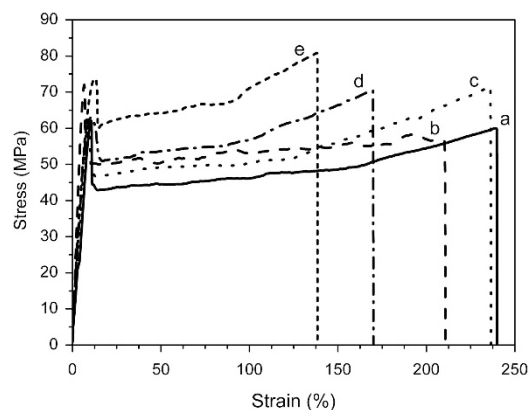


**Figure 5** Stress–strain curves of PPS/PPSU blends and their component polymers ((a)–(e): the same as Figures 4).

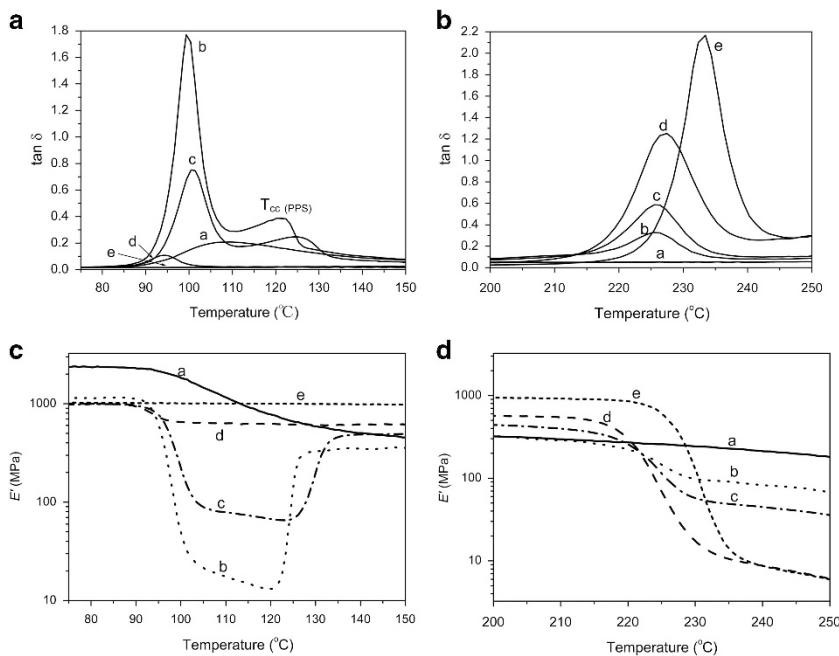


**Figure 4** (a)  $\tan \delta$  peaks of PPS, PPSU and PPS/PPSU blends measured by DMA at a heating rate of  $2$  °C  $\text{min}^{-1}$ , 1 Hz near  $T_g(\text{PPS})$ . (b)  $\tan \delta$  peaks of PPS, PPSU and PPS/PPSU blends measured by DMA at a heating rate of  $2$  °C  $\text{min}^{-1}$ , 1 Hz near  $T_g(\text{PPSU})$  ((PPS)/(PPSU) weight ratio of (a) (100/0), (b) (70/30), (c) (50/50), (d) (30/70), (e) (0/100)). (c) Storage modulus,  $E'$ , of PPS, PPSU and PPS/PPSU blends measured by DMA at a heating rate of  $2$  °C  $\text{min}^{-1}$ , 1 Hz near  $T_g(\text{PPS})$ . (d) Storage modulus,  $E'$  of PPS, PPSU and PPS/PPSU blends measured by DMA at a heating rate of  $2$  °C  $\text{min}^{-1}$ , 1 Hz near  $T_g(\text{PPSU})$  ((PPS)/(PPSU) weight ratio of (a) (100/0), (b) (70/30), (c) (50/50), (d) (30/70), (e) (0/100)).



**Table 2** Tensile properties of PPS, PPSU, and their blends

Sample	Tensile properties <sup>a</sup>			
	TM (MPa)	TS (MPa)	TB (MPa)	EB (%)
(100) PPS	1707	72	56	211
(100) PPSU	2003	80	80	197
(70/30) PPS/PPSU	690	64	63	270
(50/50) PPS/PPSU	557	71	71	236
(30/70) PPS/PPSU	502	69	69	178

Abbreviations: *EB*, elongation at break; PPS, poly(*p*-phenylene sulfide); PPSU, poly(phenylsulfone); *TB*, tensile stress at break; *TM*, tensile modulus; *TS*, tensile strength.  
<sup>a</sup>Average values of *TM*, *TS*, *TB* and *EB* were obtained by five measurements.

additivity rule applies for the yield stress, where  $\sigma$  and  $\phi$  are the yield stress and the volume fraction, respectively, and the subscripts *b*, *d* and *m* indicate the blend, the domain and the matrix, respectively.

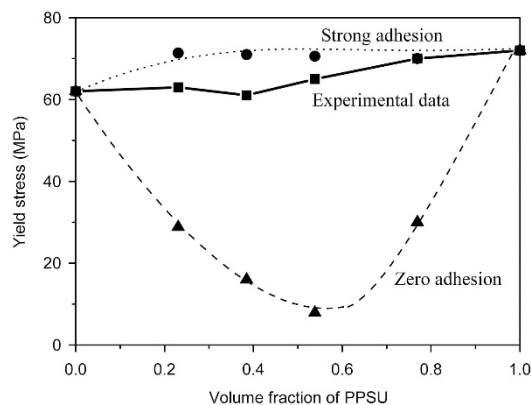
$$\sigma_b = \sigma_d \phi_d + \sigma_m \phi_m \quad (2)$$

In contrast, for a blend with no interfacial adhesion, in which the domains only reduce the load-bearing cross section of the matrix, the following equation is proposed.<sup>32</sup>

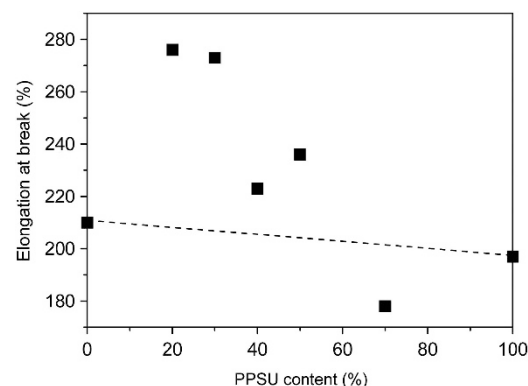
$$\sigma_b = \sigma_m \frac{1 - \phi_d}{1 + 2.5\phi_d} \quad (3)$$

Figure 6 shows the yield stress of the PPS/PPSU blends measured by the tensile tests plotted against the blend composition. The experimental data were compared with the values calculated from Equations (2) and (3). It was found that the experimental data were very close to the values calculated from Equation (2), implying that the interfacial adhesion was strong enough to ensure stress transfer between the matrix and the domains. Similar behavior has been observed for other partially miscible blends of PC/poly(methyl methacrylate)<sup>32</sup> and poly(methyl methacrylate)/poly(vinyl chloride)<sup>31</sup> In addition, a positive deviation from the additivity rule in yield stress has been observed for partially miscible blends, such as PC/poly(styrene-co-acrylonitrile), PC/poly(acrylonitrile-butadiene-styrene)<sup>33</sup> and poly(propylene carbonate)/poly(lactic acid),<sup>32</sup> in which it was surmised that the molecular mobilities of the component polymers were suppressed due to the associative interactions between the different polymers.<sup>33</sup> In a well-known miscible blend of poly(phenylene ether)/PS, a large positive deviation from the additivity rule was observed, whereas in an incompatible blend of polypropylene/poly(vinyl chloride) assumed to have zero adhesion at the interface, the change in the yield stress followed Equation (3).<sup>31,34</sup>

Furthermore, the elongation at break of the PPS/PPSU blends showed a positive deviation from the additivity rule against the blend composition, except for the (30/70) PPS/PPSU, as demonstrated in Figure 7. There are two possible causes for the increase in the elongation at break: first, the desirable interfacial adhesion achieved by the partial miscibility sustained stress transfer to the tensile fracture; second, a change in crystallinity and in the crystalline structure caused by stretching contributed to the enhancement of the elongation at break. Here, the segmental mobility of PPSU, observed as a transition peak at approximately  $-100^\circ\text{C}$  in the DMA measurements, most likely contributed to the dissipation of the energy imposed by the external stress at room temperature. The observation of a locus of failure also supports the presence of good interfacial adhesion. Furthermore, in the PPS/PPSU blends,



**Figure 6** Yield stress versus the volume fraction of PPSU in PPS/PPSU blends (■: experimental data and predicted values; ●: from Equation (2) and ▲: from Equation (3)).



**Figure 7** Elongation at break versus PPSU content in PPS/PPSU blends measured by tensile tests.

the higher the PPSU content, the lower the tensile modulus although the tensile modulus of neat PPSU is higher than that of neat PPS, as shown in Table 2.

#### Crystallization of PPS in the PPS/PPSU blends

Attempts were made to elucidate the effects of the partial miscibility between PPS and PPSU on the crystallization of PPS. Figures 8a and b show DSC thermograms of neat PPS and the (50/50) PPS/PPSU blend, respectively, measured during cooling at various rates from the molten state. It was demonstrated that the melt crystallization of the blend shifted to a temperature  $22\text{--}27^\circ\text{C}$  lower than that of neat PPS at the same cooling rate. In addition, the peak area and sharpness of the peaks were significantly reduced upon blending. These results imply that the partial miscibility of PPSU with PPS interferes with the crystallization of PPS and suppresses the regularity in the PPS crystalline structure. The suppression of PPS crystallization by blending has also been observed in PPS/PC<sup>17</sup> and PPS/high-density polyethylene.<sup>14</sup> The effect of suppression by blending has also been observed in PPS/high-impact PS<sup>15</sup> and in PPS/thermotropic liquid crystalline polymer,<sup>10</sup> although these studies did not mention partial miscibility.

Some blends have been described in which the crystallization of PPS was not affected by the presence of another polymer component, for example, in PPS/polysulfone (PSF)<sup>35</sup> and PPS/PEEK.<sup>21</sup> Both PSF

and PEEK are amorphous and completely immiscible with PPS. Furthermore, it has been reported that another polymer incorporated into PPS can function as a nucleating agent and/or accelerate the crystallization rate of PPS, for example, in PPS/poly(ether imide),<sup>13</sup> PPS/PA6,<sup>7</sup> PPS/PA66<sup>5</sup> and PPS/PET.<sup>14</sup> Crystallization in immiscible polymer blends is often affected by nucleation at the interface and by the rejection, engulfment and deformation of the second component by the crystallizing polymer, which are governed by several factors, such as the relative melt viscosity, chemical compatibility, miscibility, composition, and morphology.<sup>14</sup>

Next, the effects of PPSU on the interlamellar structure of PPS were examined by SAXS, as shown in Figure 9. The crystal lamellar thickness ( $l_c$ ) and the amorphous layer thickness ( $l_a$ ) were calculated based on a dual phase model.<sup>36</sup> The value of  $l_c$  was found to be 3.8 nm for neat PPS, which significantly decreased upon the addition of PPSU to 1.8 nm and 1.1 nm in the blends containing 15 wt% and 50 wt% PPSU, respectively. In contrast, the long period,  $l_c + l_a$ , of the PPS crystallites significantly increased, from 15.7 nm to over 20 nm, upon the addition of 5 wt% PPSU, which was solely caused by an increase in the amorphous component between the PPS lamellae. In the literature, the long period and the value of  $l_c$  of neat PPS with a viscosity average molecular weight of 30 000 g mol<sup>-1</sup> are reported to be, respectively, 13 nm and ~3 nm at 19% crystallinity,<sup>37</sup> and those of

a PPS oligomer are reported to be ~10 nm and ~5 nm at 47% crystallinity,<sup>38</sup> respectively. Both values are in reasonable agreement with our results.

The crystallization in crystalline/amorphous blends usually involves two types of polymer transport: in the first, the crystalline polymer component diffuses toward the crystal growth front, and in the second, the amorphous polymer component segregates away from the growth front.<sup>39</sup> The suppression of PPS crystallization is most likely caused by disturbances in the first transport, in which the PPSU chains prevent the PPS chains from migrating toward the crystal growth front. Furthermore, it is considered that the second transport results in the expulsion of the amorphous polymer into the interlamellar, interfibrillar or interspherulitic regions.<sup>40</sup> In the present PPS/PPSU blend, the interlamellar segregation of the<sup>41–43</sup> amorphous polymer occurred during the crystallization of PPS, which resulted in a significant increase in  $l_a$ . The insertion of the PPSU chains between the PPS lamellae caused a decrease in the regularity of the PPS crystalline structure and led to the prevention of PPS crystallization at higher PPSU contents, as demonstrated by the DSC results shown in Figures 8a and b. The same phenomenon was also reported in a miscible blend of poly(lactic acid)/poly(4-vinylphenol).<sup>39</sup>

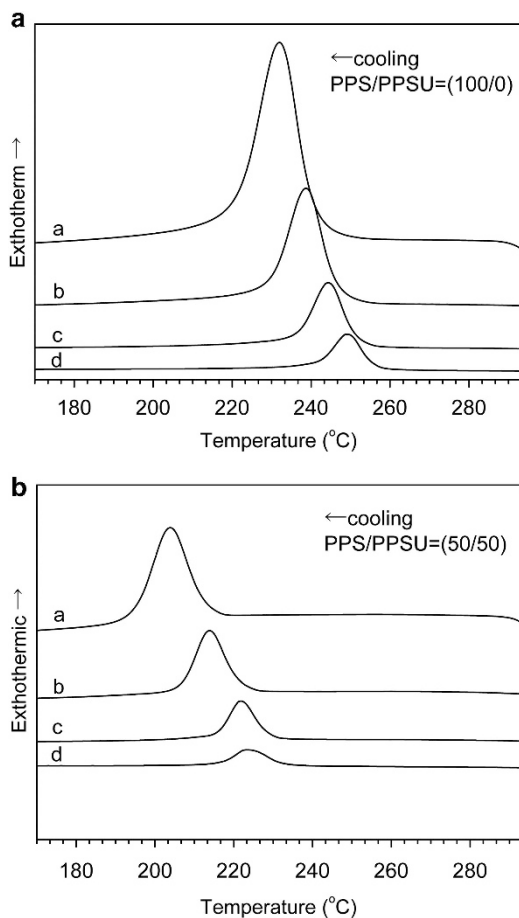


**Figure 8** (a). DSC thermograms of neat PPS measured at various cooling rates ((a) 40 °C min<sup>-1</sup>, (b) 20 °C min<sup>-1</sup>, (c) 10 °C min<sup>-1</sup>, (d) 5 °C min<sup>-1</sup>). (b) DSC thermograms of the (50/50) PPS/PPSU blend measured at various cooling rates ((a) 40 °C min<sup>-1</sup>, (b) 20 °C min<sup>-1</sup>, (c) 10 °C min<sup>-1</sup>, (d) 5 °C min<sup>-1</sup>).

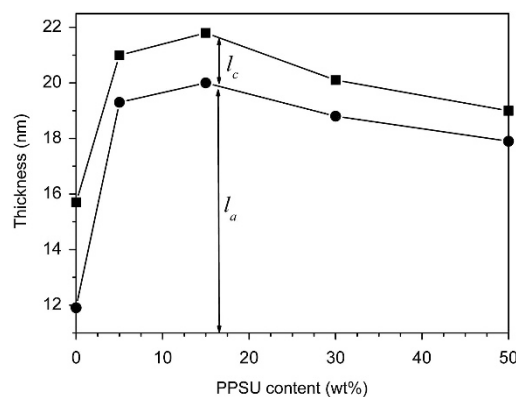


**Figure 9** Average long period (■) and amorphous part thickness ( $l_a$ ) (●) of neat PPS and PPS/PPSU blends estimated by SAXS ( $l_c$  = average crystalline thickness).

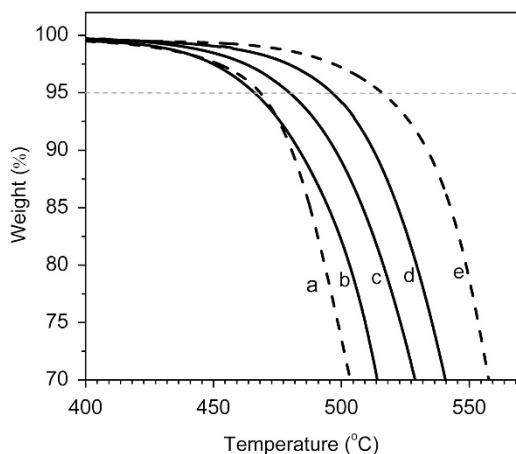


**Figure 10** Decomposition behavior of PPS, PPSU and PPS/PPSU blends during heating in N<sub>2</sub> at a heating rate of 10 °C min<sup>-1</sup> measured by TGA ((PPS)/(PPSU) weight ratio of (a) (100/0), (b) (70/30), (c) (50/50), (d) (30/70), (e) (0/100)).

**Table 3 Thermal stabilities of PPS, PPSU and their blends**

Sample	Decomposition temperature <sup>a</sup> (°C)
PS	468
PPSU	516
(70/30) PPS/PPSU	466
(50/50) PPS/PPSU	480
(30/70) PPS/PPSU	496

Abbreviations: PPS, poly(*p*-phenylene sulfide); PPSU, poly(phenylsulfone).

<sup>a</sup>Decomposition temperature estimated as temperature observed at 5 wt% loss.

### Thermal stability

Finally, the thermal stability of PPS/PPSU at various compositions was investigated. Figure 10 shows TGA data obtained under a nitrogen atmosphere. The temperature observed at 5% weight loss is listed as the decomposition temperature in Table 3 and was used as the criterion for the onset of polymer decomposition. As shown in the table, the thermal stability of PPSU is extremely high at 516 °C, so that the thermal stabilities of the PPS blends were significantly improved upon the addition of PPSU; the higher the PPSU content, the higher the decomposition temperature. For example, although (30/70) PPS/PPSU consists of the PPS matrix with a lower thermal stability, its decomposition temperature was as high as ~500 °C, which is ~30 °C higher than that of neat PPS.

### CONCLUSIONS

Blends composed of two super-engineering plastics, poly(*p*-phenylene sulfide) (PPS)/poly(phenylsulfone) (PPSU), were studied in detail by various techniques, including DSC, DMA, small-angle X-ray scattering (SAXS), TGA, transmission electron microscopy (TEM) and tensile tests. It was found from the DSC and DMA measurements that PPSU was partially miscible with PPS in the blend acting as an inhibitor of PPS crystallization.

Furthermore, the SAXS measurements revealed that the long period and the amorphous layer thickness of the PPS crystallites significantly increased upon the addition of PPSU, indicating the intrusion of the PPSU chains into the amorphous regions between the PPS lamellae as a result of the interlamellar segregation of the PPSU chains during PPS melt-crystallization. It was demonstrated that the desirable interfacial adhesion achieved by the partial miscibility sustained stress transfer to the tensile fracture. It was presumed that the segmental mobility of PPSU observed at approximately -100 °C in the DMA measurements would efficiently contribute to the dissipation of the energy imposed by external stress at room temperature. Moreover, TGA measurements under a nitrogen atmosphere demonstrated that the thermal stabilities of the PPS blends were significantly improved upon the addition of PPSU.

### ACKNOWLEDGEMENTS

Financial support was kindly provided by the Japan Society for the Promotion of Science (JSPS) Kakenhi Grant Number 22605006 and the Supported Program for the Strategic Research Foundation at Private Universities provided by the Ministry of Education, Culture, Sports, Science and Technology of Japan. The authors are deeply thankful to the BASF Corporation, Germany, and the Kureha Corporation, Japan, for kindly providing us with the PPSU and PPS samples, respectively. The TEM micrograph was kindly taken by S Shida at the IMU Cooperative Research Center of Iwaki Meisei University, Japan.

- Kurihara, F. (ed.) in: *Encyclopedia of Polymeric Materials*, Vol. 300 (Nikkan Kogyo, Tokyo, 1999).
- Committee of Encyclopedia of plastic functional polymer materials. (Ed.) *Encyclopedia of Plastic Functional Polymer Materials* (Sunchoh publishing, Tokyo, Japan, 2004).
- Hergenrother, P. M. (ed.) in: *Advances in Polymer Science*, Vol. 117 (Springer-Verlag, Berlin, 1994).
- Wu, B., Zheng, X., Leng, J. H., Yang, B., Chen, X. & He, B. B. Compatibilization of ethylene/maleic anhydride/glycidyl methacrylate terpolymer for poly(phenylene sulfide)/poly(amide-66) Blends. *J. Appl. Polym. Sci.* **124**, 325–332 (2012).
- Zhang, R. C., Huang, Y. G., Min, M., Gao, Y., Lu, A. & Lu, Z. Y. Nonisothermal crystallization of polyamide 66/poly(phenylene sulfide) blends. *J. Appl. Polym. Sci.* **107**, 2600–2606 (2008).
- An, J. B., Suzuki, T., Ougizawa, T., Inoue, T., Mitamura, K. & Kawanishi, K. Studies on miscibility and phase-separated morphology of nylon 4,6/poly(phenylene sulfide) blend under shear flow. *J. Macromol. Sci. B Phys.* **41**, 407–418 (2002).
- Mai, K. C., Chang, S. C., Gao, Q. F. & Zeng, H. M. Effect of interface on crystallization behavior of polyphenylene sulfide blends with polyamide 6. *Act. Polym. Sin.* **1**, 121–123 (2001).
- Tang, W. H., Hu, X. Y., Tang, J. & Jin, R. G. Toughening and compatibilization of polyphenylene sulfide/nylon 66 blends with SEBS and maleic anhydride grafted SEBS triblock copolymers. *J. Appl. Polym. Sci.* **106**, 2648–2655 (2007).
- Rath, T., Kumar, S., Mahaling, R. N., Das, C. K. & Yadaw, S. B. Mechanical and morphological study of polyphenylene sulfide/liquid crystalline polymer blends compatibilized with a maleic anhydride grafted copolymer. *J. Appl. Polym. Sci.* **106**, 3721–3728 (2007).
- Gopakumar, T. G., Ghadage, R. S., Ponrathnam, S., Rajan, C. R. & Fradet, A. Poly(phenylene sulfide)/liquid crystalline polymer blends. 1: Non-isothermal crystallization kinetics. *Polymer* **38**, 2209–2214 (1997).
- Masamoto, J. & Kubo, K. Elastomer-toughened poly(phenylene sulfide). *Polym. Eng. Sci.* **36**, 265–270 (1996).
- Hisamatsu, T., Nakano, S., Adachi, T., Ishikawa, M. & Iwakura, K. The effect of compatibility on toughness of pps/sebs polymer alloy. *Polymer*, **41**, 4803–4809 (2000).
- Wu, X. S., Wei, H. B., Zhu, J. & Fang, X. Z. Study on thermal properties and crystallization behavior of blends of poly(phenylene sulfide)/poly(ether imide). *Polym. Plast. Technol.* **49**, 1506–1514 (2010).
- Jog, J. P., Shingankuli, V. L. & Nadkarni, V. M. Crystallization of poly(phenylene sulfide) in blends with high-density polyethylene and poly(ethylene-terephthalate). *Polymer* **34**, 1966–1969 (1993).
- Zhang, R. C., Lu, A., Min, M., Lu, Z. Y. & Huang, Y. G. Non-isothermal crystallization of high-impact polystyrene/poly(phenylene sulfide) blends. *Polym. Plast. Technol.* **47**, 215–222 (2008).
- Quan, H., Li, Z. M., Yang, M. B. & Lu, Z. Y. Nonisothermal crystallization nucleation of *in situ* fibrillar and spherical inclusions in poly(phenylene sulfide)/isotactic polypropylene blends. *J. Macromol. Sci. B Phys.* **44**, 761–778 (2005).
- Wu, D., Zhang, Y., Zhang, M. & Wu, L. Morphology, nonisothermal crystallization behavior, and kinetics of poly(phenylene sulfide)/polycarbonate blend. *J. Appl. Polym. Sci.* **105**, 739–748 (2007).
- Shibata, M., Yosomiya, R., Jiang, Z., Yang, Z., Wang, G., Ma, R. & Wu, Z. Crystallization and melting behavior of poly(*p*-phenylene sulfide) in blends with poly(ether sulfone). *J. Appl. Polym. Sci.* **74**, 1686–1692 (1999).
- Lai, M. F., Yang, Y. M. & Liu, J. J. Reactive reinforcement of the interface of poly(ether sulfone)/poly(phenylene sulfide) polymer blend by PMR-POI. *J. Appl. Polym. Sci.* **85**, 1297–1306 (2002).
- Zhang, R. C., Xu, Y., Lu, Z. Y., Min, M., Gao, Y., Huang, Y. G. & Lu, A. Investigation on the crystallization behavior of poly(ether ether ketone)/poly(phenylene sulfide) blends. *J. Appl. Polym. Sci.* **108**, 1829–1836 (2008).
- Mai, K., Mei, Z., Xu, J. & Zeng, H. Effect of blending on the multiple melting behavior of polyphenylene sulfide. *J. Appl. Polym. Sci.* **63**, 1001–1008 (1997).
- Harris, J. E. & Brooks, G. T. *Process for Miscible Blends of Imide Containing Polymers with Poly(aryl sulfones)* Amoco Corp. US Patent, US 5134202 (1992).
- Retolaza, A., Eguiazabal, J. I. & Nazabal, J. Structure and properties of compatible PPSF-rich blends with PET. *Macromol. Mater. Eng.* **289**, 708–713 (2004).
- Di Vona, M. L., D'Epifanio, A., Marani, D., Trombetta, M., Traversa, E. & Licocchia, S. SPEEK/PPSU-based organic-inorganic membranes: proton conducting electrolytes in anhydrous and wet environments. *J. Membrane Sci.* **279**, 186–191 (2006).
- Weng, T. H., Tseng, H. H. & Wey, M. Y. Preparation and characterization of PPSU/PBNPI blend membrane for hydrogen separation. *Int. J. Hydrogen Energ.* **33**, 4178–4182 (2008).
- Sun, H., Mark, J. E., Tan, S. C., Venkatasubramanian, N., Houtz, M. D., Arnold, F. E. & Lee, C. Y-C. Microcellular foams from some high-performance composites. *Polymer* **46**, 6623–6632 (2005).
- Brandrup, J., Immergut, E. H. & Grulke, E. A. (eds) *Polymer Handbook*. 4th Edn, Vol. 1, pVI/58 (Wiley-Interscience, Hoboken, NJ, 1999).
- Oyama, H. T., Sekikawa, M. & Ikezawa, Y. Influence of the polymer/inorganic filler interface on the mechanical, thermal, and flame retardant properties of polypropylene/magnesium hydroxide composites. *J. Macromol. Sci. B Phys.* **50**, 463–483 (2011).
- Wade, B., Abhiraman, A. S., Wharry, S. & Sutherland, D. High-temperature, high-resolution nuclear-magnetic-resonance of poly(para-phenylene sulfide). *J. Polym. Sci. B Polym. Phys.* **28**, 1233–1249 (1990).
- Macosko, C. W. Morphology development and control in immiscible polymer blends. *Macromol. Symp.* **149**, 171–184 (2000).

- 31 Kolařík, J., Lednický, F., Pukánszky, B. & Pegoraro, M. Blends of polycarbonate with poly(methyl methacrylate)—miscibility, phase continuity, and interfacial adhesion. *Polym. Eng. Sci.* **32**, 886–893 (1992).
- 32 Ma, X. F., Yu, J. G. & Wang, N. Compatibility characterization of poly(lactic acid)/poly(propylene carbonate) blends. *J. Polym. Sci. B Polym. Phys.* **44**, 94–101 (2006).
- 33 Kolařík, J. Positive deviations of the modulus and yield strength of blends consisting of partially miscible polymers. *J. Macromol. Sci. B Phys.* **39**, 53–66 (2000).
- 34 Fekete, E., Földes, E., Damsits, F. & Pukánszky, B. Interaction-structure-property relationships in amorphous polymer blends. *Polym. Bull.* **44**, 363–370 (2000).
- 35 Mai, K., Mei, Z., Xu, J. & Zeng, H. Effect of high-performance polymers on crystallization and multiple melting behavior of poly(phenylene sulfide). *J. Appl. Polym. Sci.* **69**, 637–644 (1998).
- 36 Strobl, G. R. & Schneider, M. Direct evaluation of the electron-density correlation-function of partially crystalline polymers. *J. Polym. Sci. Polym. Phys.* **18**, 1343–1359 (1980).
- 37 Lu, S. X., Cebe, P. & Capel, M. Effects of molecular weight on the structure of poly(phenylene sulfide) crystallized at low temperatures. *Macromolecules* **30**, 6243–6250 (1997).
- 38 Sass, C. S. & Fagerburg, D. R. Optical and SAXS characterization of poly(phenylene sulfide)(PPS) oligomers. *J. Polym. Sci. B Polym. Phys.* **32**, 579 (1994).
- 39 Chen, H. L., Liu, H. H. & Lin, J. S. Microstructure of semicrystalline poly(L-lactide)/poly(4-vinylphenol) blends evaluated from SAXS absolute intensity measurement. *Macromolecules* **33**, 4856–4860 (2000).
- 40 Russell, T. P., Ito, H. & Wignall, G. D. Neutron and x-ray-scattering studies on semicrystalline polymer blends. *Macromolecules* **21**, 1703–1709 (1988).
- 41 Graebling, D., Muller, R. & Palierne, J. F. Linear viscoelastic behavior of some incompatible polymer blends in the melt—interpretation of data with a model of emulsion of viscoelastic liquids. *Macromolecules* **26**, 320–329 (1993).
- 42 Bousmina, M., Palierne, J. F. & Utracki, L. A. Modeling of structured polyblend flow in a laminar shear field. *Polym. Eng. Sci.* **39**, 1049–1059 (1999).
- 43 Shan, C. L. P., Soares, J. B. P. & Penlidis, A. HDPE/LLDPE reactor blends with bimodal microstructures - part ii: rheological properties. *Polymer* **44**, 177–185 (2003).